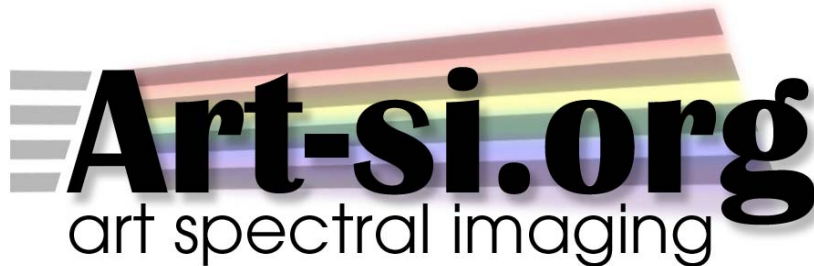


**Technical Report**

**Evaluation of Optical Flare and Its Effects On Spectral  
Estimation Accuracy**

**February 25, 2003**



**David C. Day**

**Spectral Color Imaging Laboratory Group  
Munsell Color Science Laboratory  
Chester F. Carlson Center for Imaging Science  
Rochester Institute of Technology**

[dcd7078@cis.rit.edu](mailto:dcd7078@cis.rit.edu)

<http://www.art-si.org/>

## **Introduction:**

Currently, one of the major goals of the Spectral Color Imaging Laboratory at the Munsell Color Science Laboratory is the creation of a spectral imaging system in order to create accurate image archives and lay the groundwork for methods to create non-metameric image reproductions. While many aspects of the imaging chain have been accounted for, one aspect that requires further investigation is optical flare. This technical report will focus on image acquisition and the need to reduce flare in order to create a mathematical transform which will accurately convert camera digital counts (input) into estimated values of spectral reflectance (output).

Optical flare (referred to as flare for the remainder of this report) is defined as non-image forming light incident on the detector plane (Stroebe, *et al.*). It is a result of extraneous reflections present in the scene and caused by the optics of the system. Flare from scene reflections can be reduced in many ways, such as covering highly reflective objects not relevant to the scene, positioning of the light sources, etc. In the following experiment, reflection targets were imaged five times with flare being reduced incrementally. The captured images were then used to develop the transforms that convert the digital data obtained from the camera into estimates of spectral reflectance.

## **Experimental:**

Figure 1 illustrates the basic setup of the scene and shows what was done to reduce flare incrementally. The setup was made so that, initially, it would contain a great deal of flare and would give a baseline to show the improvement in the spectral estimation accuracy as flare was reduced (Flare 1). Unimportant objects that were either part of the scene or exposed to the lighting included a linoleum tile floor and a white eraser board in the background. Flare 2 added a backdrop behind the reflection target. In Flare 3, the linoleum floor directly in front of the camera was covered and in Flare 4, the eraser board was also covered. Finally, in Flare 5, a lens hood was added to the camera.

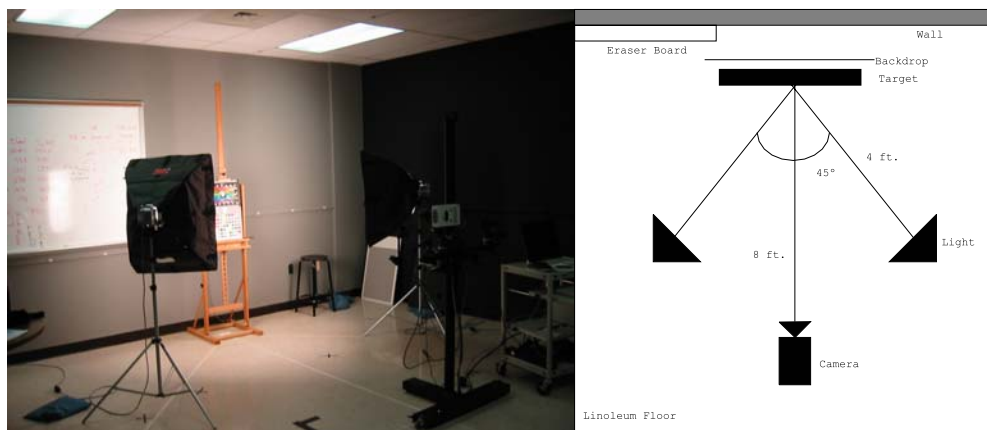


Figure 1a: Flare 1 setup

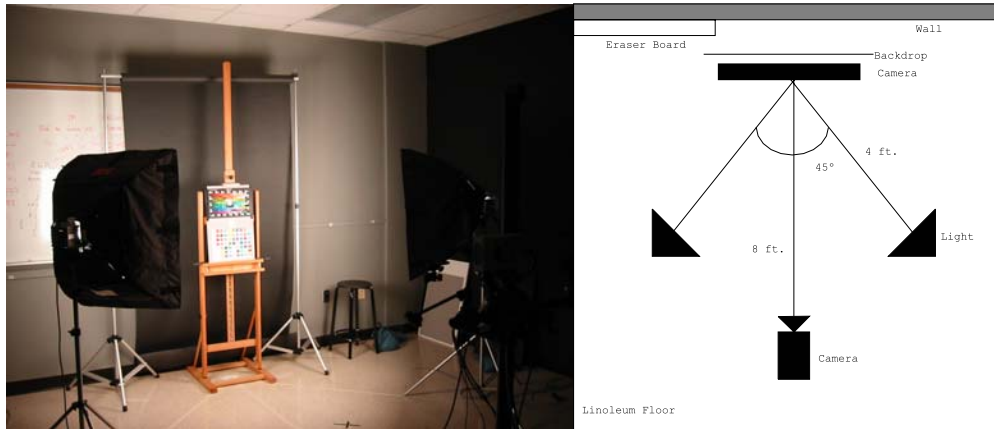


Figure 1b: Flare 2 setup

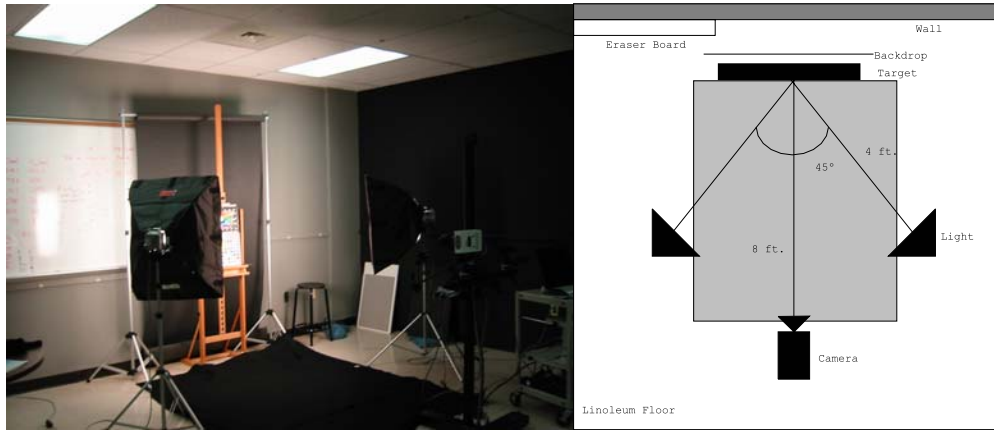


Figure 1c: Flare 3 setup



Figure 1d: Flare 4 setup

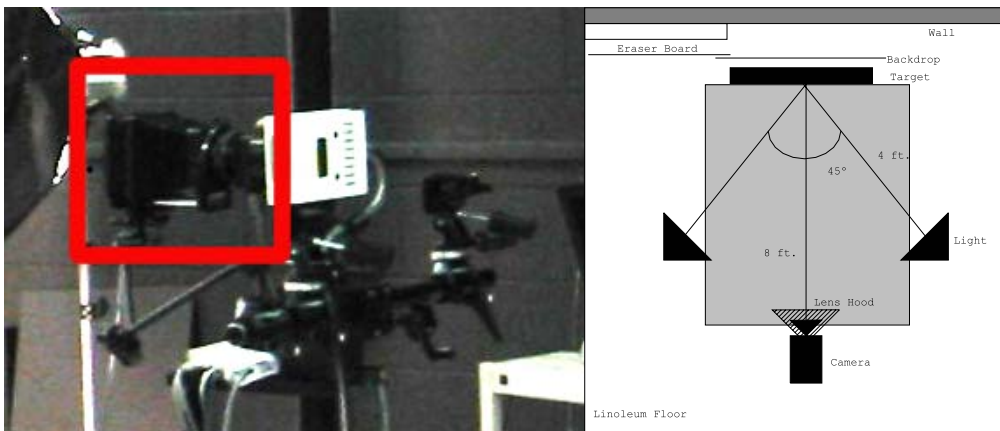


Figure 1e: Flare 5 setup

The camera used was a Roper Scientific Photometrics Quantix camera capable of producing extremely low noise 2048 X 3072 12 bit images. A computer controlled Liquid Crystal Tunable filter (LCTF) from Cambridge Research & Instrumentation (CRI) was attached to the front of the camera. Figure 2 shows a picture of the camera and LCTF. Figure 3 gives the transmittance of the LCTF at various wavelengths.

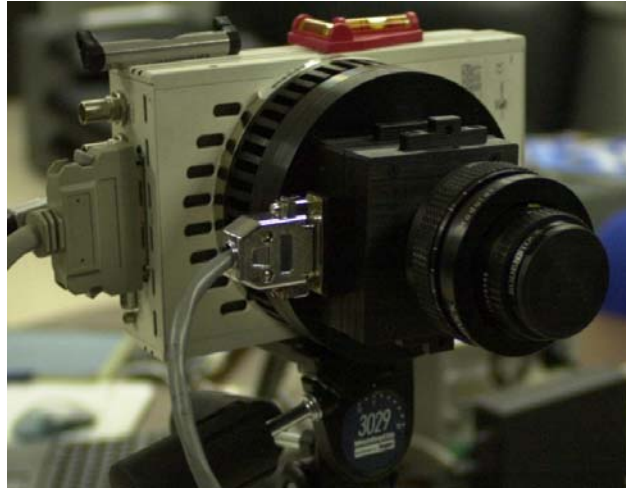


Figure 2: Quantix CCD camera and CRI LCTF

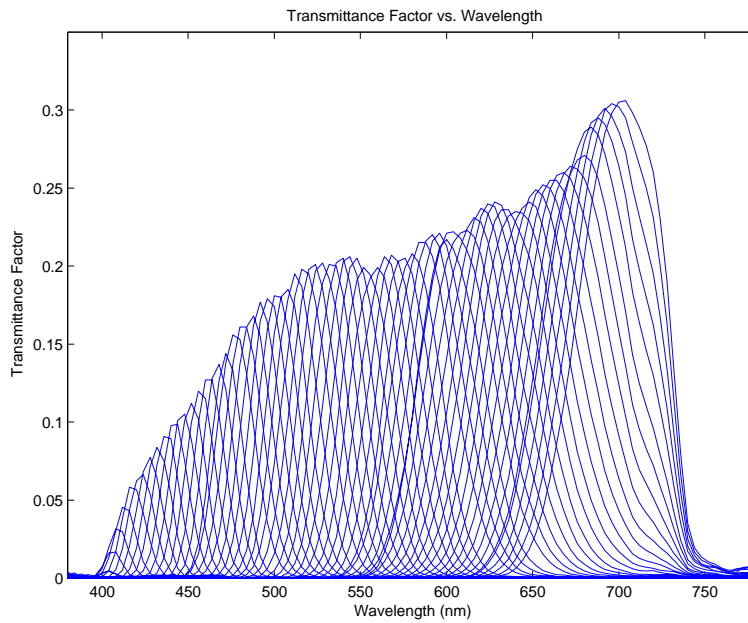


Figure 3: Transmittance of the LCTF at various wavelengths

The lens used was a 105 mm Rodenstock enlarger lens with a modular focusing mechanism. For this experiment, the system was characterized with a GretagMacbeth ColorChecker DC (CCDC) with known reflectance values from measurements made with a Spectrolino 45/0 spectrophotometer and a white halon disc used for exposure control. In order to verify the accuracy of the system after characterization, a set of patches painted using Gamblin conservation paints were used (Figure 4).



Figure 4: Reflectance Targets

Spatial correction was performed using gray cards made of Coloraid Neutral paper to approximate a uniform field. Two Elinchrome Scanlite Digital 1000 Studio lights fitted with Chimera Pro Video light diffusers were mounted on light stands and placed approximately 45 degrees to the camera's optical axis, aimed at the center of the target and placed four feet away to provide even illumination. Figure 5 gives the relative spectral power distribution of the lights as measured with a Photo Research PR-650 SpectraScan spectroradiometer.

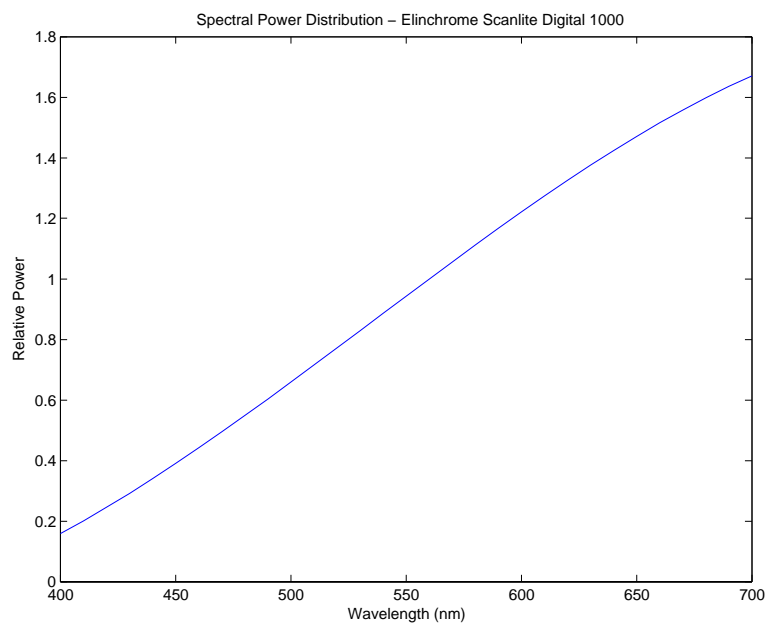


Figure 5: Spectral Power Distribution of the Elinchrome Scanlite Digital 1000

## Imaging and Data Processing:

The impact of reducing flare was tested using the processing pipeline in place at the time of the experiment. The process is divided into five major steps, shown in Figure 6. Further details can be found in the technical report by Imai *et al.*

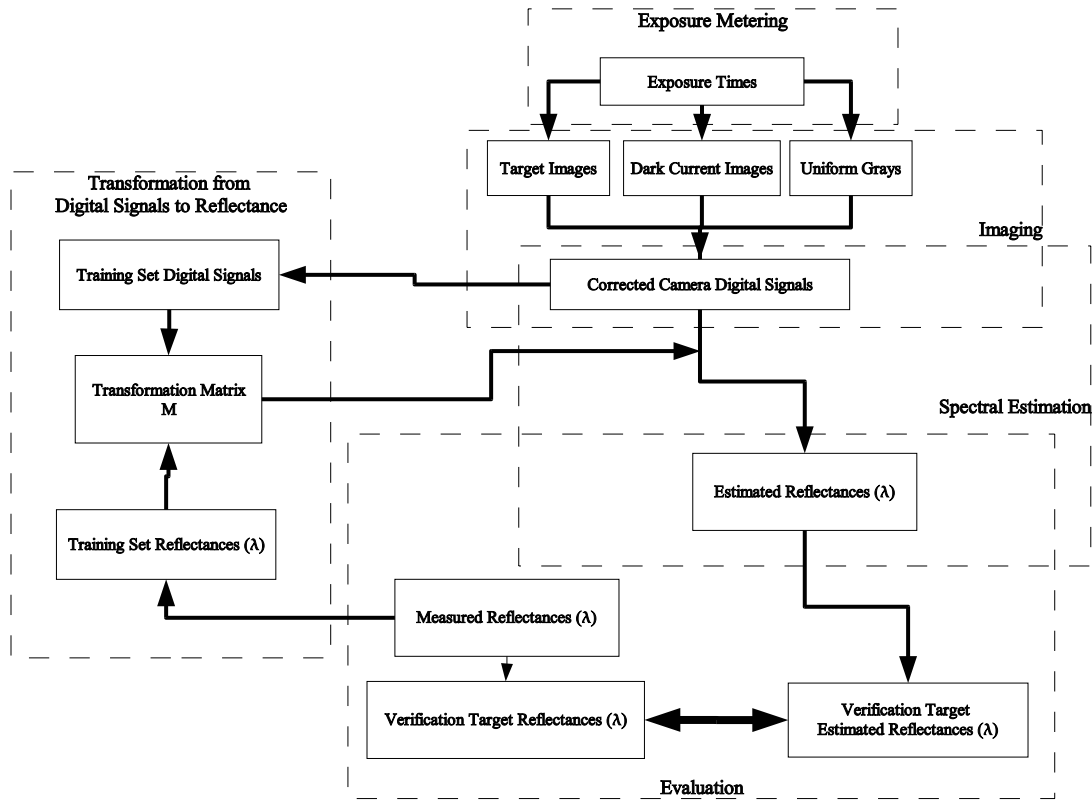


Figure 6: Processing Pipeline

## Exposure Metering:

A 31 band spectral image was created by centering the LCTF 31 times over the range of 400 to 700 nm in 10 nm increments. Using a halon disc to approximate a perfect reflecting diffuser, a time was found with the lens set at  $f/11$  using an iterative process such that the average pixel value of the disc fell within the range of [3750, 3850] with the optimal exposure considered to correspond to a digital count of 3800. This value utilized 92% of the 12 bit dynamic range, while still allowing for some variations before clipping, caused by specular highlights.

## Imaging:

The times determined for each particular scene were used to define 31 image planes. Gray card images were also recorded for each wavelength as well as the dark images (images generated with the shutter closed in order to remove fixed pattern noise from the camera). Finally, the corrected pixel values were created by subtracting the dark image and normalizing to account for non-uniformities in the lighting (Equation 1.1).

$$d = \frac{d_{\text{image}} - d_{\text{dark}}}{d_{\text{gray}} - d_{\text{dark}}} * \overline{d_{\text{gray}}} \quad (1.1)$$

### Transformation Matrix generation:

The corrected digital counts from the CCDC were used to create a pseudo-inverse transform that converted camera digital counts to spectral reflectance factor. The transform minimized the error between estimated and measured reflectance of the CCDC and was created using a method that takes clusters of image pixels from each measured sample to create robust transforms incorporating camera variability (Imai, et al).

$$\mathbf{d} = \begin{bmatrix} d_{\lambda_{400},1} & \cdots & d_{\lambda_{400},k} \\ \vdots & \ddots & \vdots \\ d_{\lambda_{700},1} & \cdots & d_{\lambda_{700},k} \end{bmatrix}$$
$$\mathbf{r} = \begin{bmatrix} r_{\lambda_{400},1} & \cdots & r_{\lambda_{400},k} \\ \vdots & \ddots & \vdots \\ r_{\lambda_{700},1} & \cdots & r_{\lambda_{700},k} \end{bmatrix} \quad (1.2)$$

$$\mathbf{M} = \mathbf{r} \mathbf{d}^\dagger$$

$$\text{where } \mathbf{M} = \begin{bmatrix} M_{1,1} & \cdots & M_{1,31} \\ \vdots & \ddots & \vdots \\ M_{31,1} & \cdots & M_{31,31} \end{bmatrix}$$

Matrix  $\mathbf{d}$  is the matrix of corrected digital counts of the training target (in this case the CCDC) where  $k$  is the total number of pixels used for characterization. Matrix  $\mathbf{r}$  is the reflectance matrix that associates reflectances with pixel  $k$ . Finally,  $\mathbf{M}$  is the resulting transformation matrix with  $M$  denoting the resulting coefficients, and  $\lambda$  is the wavelength from which data was taken. Here, the wavelength range was from 400 to 700 nm in 10 nm increments (31 intervals). The actual operation was performed in Matlab using the `pinv()` function to obtain the  $\mathbf{d}^\dagger$  matrix. The `pinv()` function returns the Moore-Penrose pseudo-inverse matrix.

### Spectral Estimation:

Using the transform and images captured in each setup, the spectral image with estimated spectral reflectance factor was calculated for both the characterization and verification targets.

$$\hat{\mathbf{r}} = \mathbf{M} \mathbf{d} \quad (1.3)$$

### Evaluation:

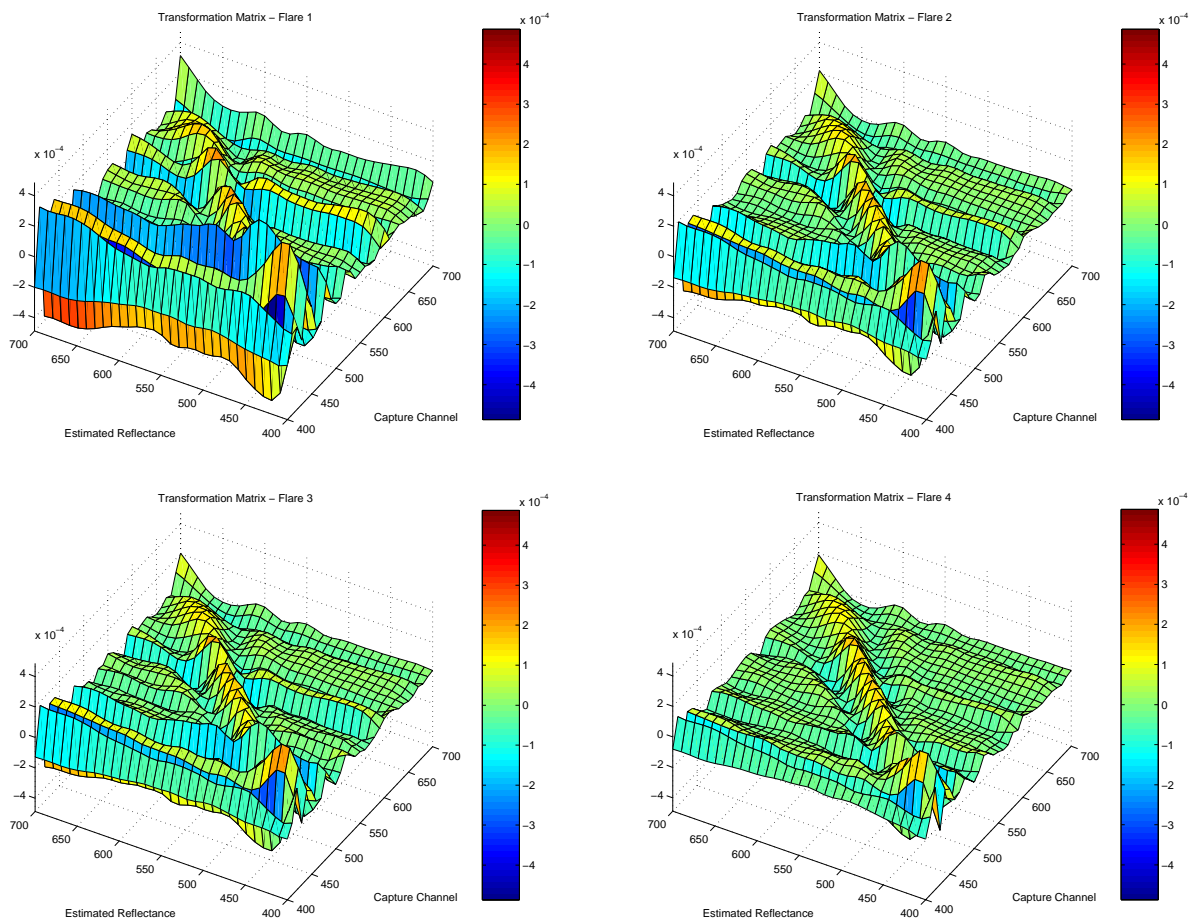
This experiment was designed to be empirical and to observe the general results of reducing flare in a scene and to show the importance of taking flare into account when performing spectral estimation. Since there is no single metric for expressing the accuracy of spectral estimation, several methods were used to show how the reduction of flare would improve the transformation matrix and spectral estimation accuracy. First, the transformation matrix coefficients were evaluated pictorially as 3-D surface plots.

Second, the colorimetric accuracy between measured and estimated reflectance was evaluated using CIELAB vector plots based on the 1931 standard observer and illuminant D65. Third, the spectral data were evaluated for representative samples. Finally, an attempt to quantify flare was made and the gray card was examined to evaluate spatial uniformity.

## **Results:**

### Visual Transformation Matrix Evaluation:

The first set of results (Figure 7) shows the graphical representations of the transformation matrices generated for flare levels 1 to 5. The transforms are showing the amount of correlation each capture channel has with the wavelength being estimated. For example, the transform from flare 1 is showing that the reflectance estimate at 700 nm will need to subtract information from the digital count obtained from the 400 nm channel. Ideally, it is expected that there will be a high correlation between a capture channel and the reflectance corresponding to that channel, resulting in a transform with a sharp diagonal and small off diagonal terms. As flare is reduced, the transform created begins to appear more like this theoretical ideal, as shown by the transform generated at flare 5.



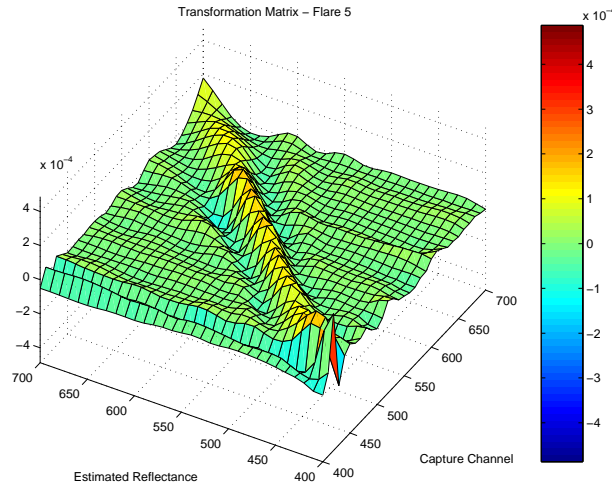
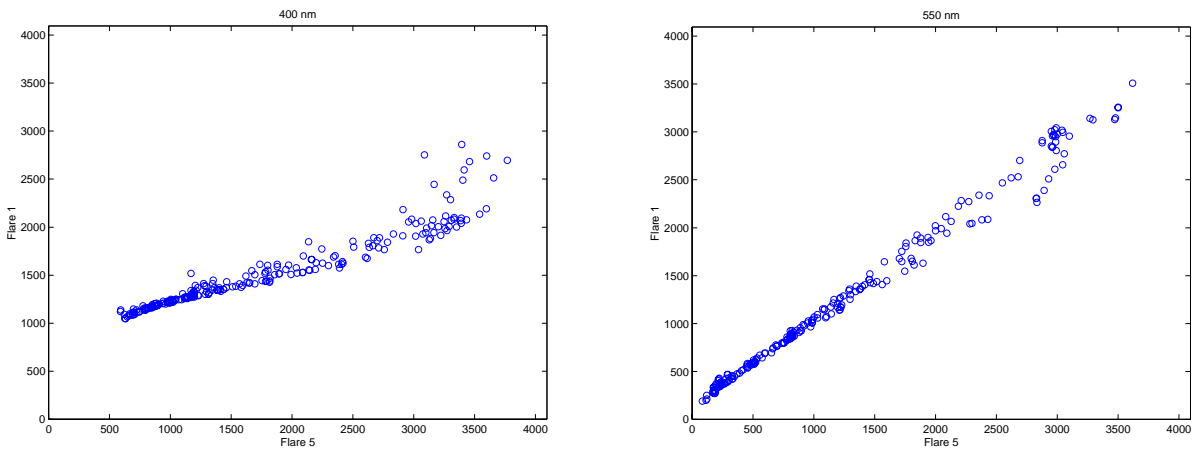


Figure 7: Transformation Matrices – Flare 1-5

To try and better understand or find factors that may be affecting the system in the lower and upper wavelengths of the transform, plots of the average digital counts of the CCDC at flare 1 vs. flare 5 were made. This is representative of plotting the best situation (flare reduced via the use of a hood and masking of certain aspects in the scene) against the worst (no attempt at reducing flare) to look for any kind of trends across wavelength. While the plots suggest that the effects of optical flare have a wavelength dependency, it is not yet certain as to why this may be happening. Figure 8 illustrates an apparent wavelength dependency of optical flare.



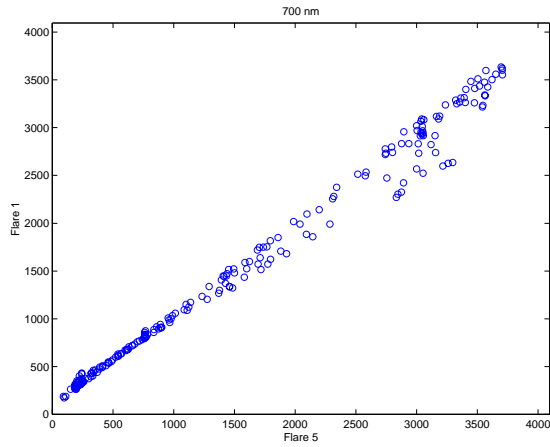


Figure 8: Flare 1 vs. Flare 5 at 400, 550 and 700 nm

At 400 nm, the grouping appears to be rather flat, suggesting very low contrast across the image and little pixel variation at flare1. At 550 nm, the points seem to have a linear relationship meaning that the flare would have less effect. At 700 nm, a linear relationship still appears to hold, but there appears to be a deviation with samples that yield a higher digital count. In the future an investigation into the factors causing this apparent dependency may be necessary.

Differences between Measured and Estimated Spectra

Figures 9a and 9b graphs the average difference between the measured and estimated spectra at each flare level for the CCDC and Gamblin paint targets. The different scales should be noted.

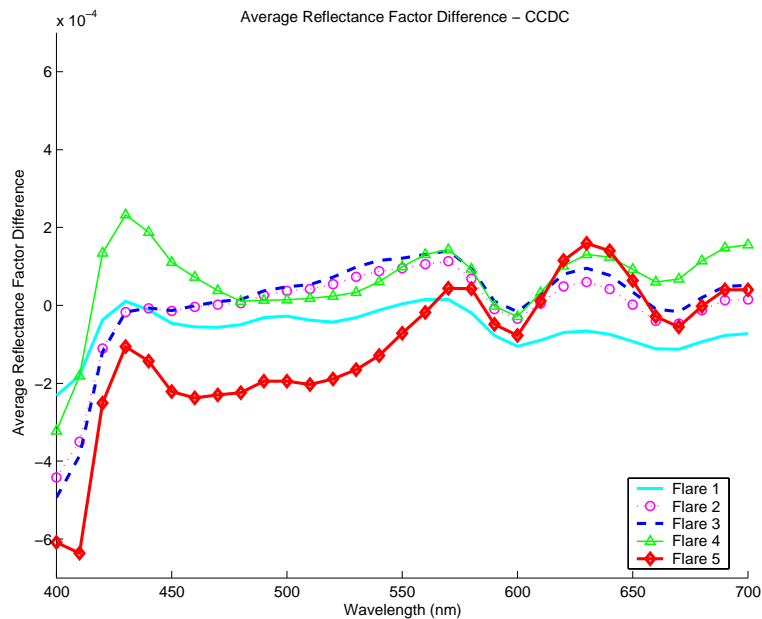


Figure 9a

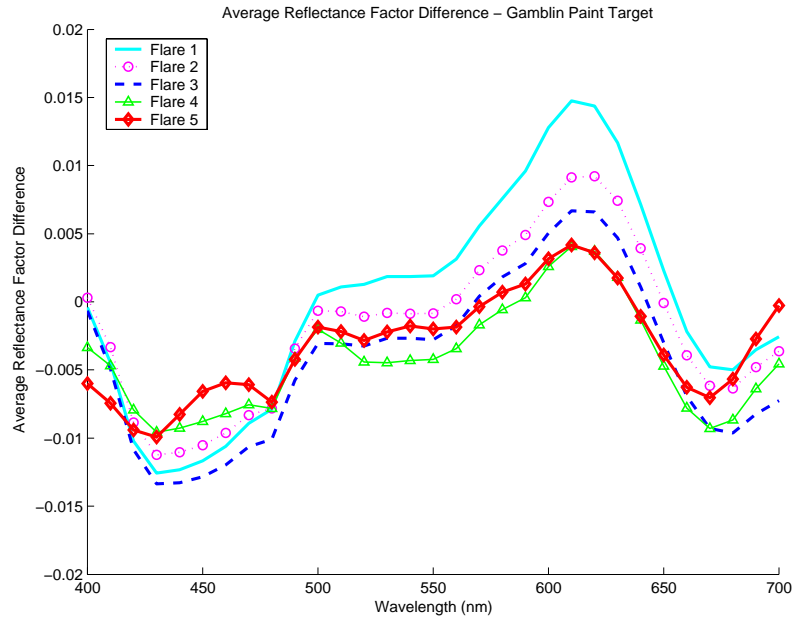


Figure 9b

As expected, the CCDC graph shows very little average difference for all the patches as all the transforms were characterized with these data. The plot of the average reflectance difference of the Gamblin samples shows that there is the most average difference in the lower and upper wavelengths, but overall gets progressively better with the reduction in flare. To look further at this phenomenon, five patches were selected from flare level one from the Gamblin target. These patches possess the most RMS Spectral error for the first flare level. Figures 10a and 10b show the measured and estimated spectra of the cobalt blue and cadmium yellow light patches, which is representative of the improving trends noticed amongst all the evaluated patches. While the general curve shape for the estimated reflectance remained the same, the flare behaved as a scaling factor.

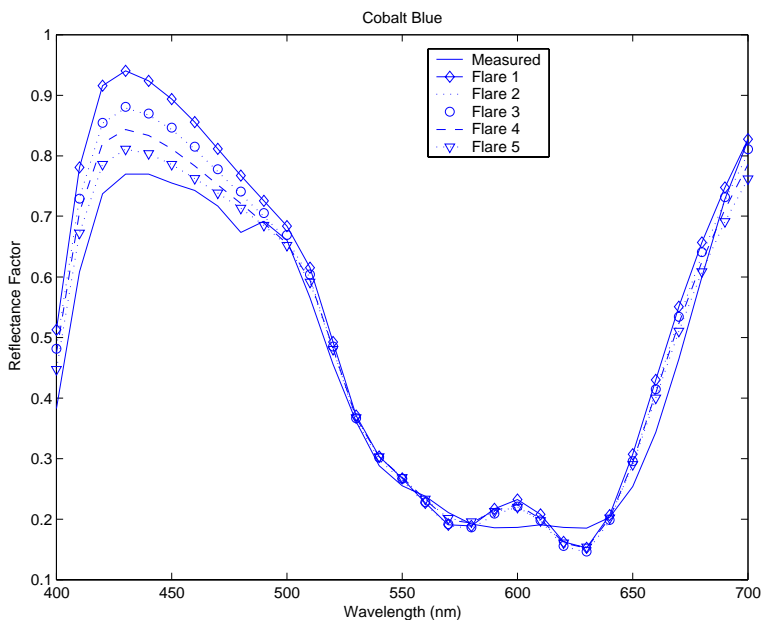


Figure 10a: Measured and Estimated Spectra for Cobalt Blue

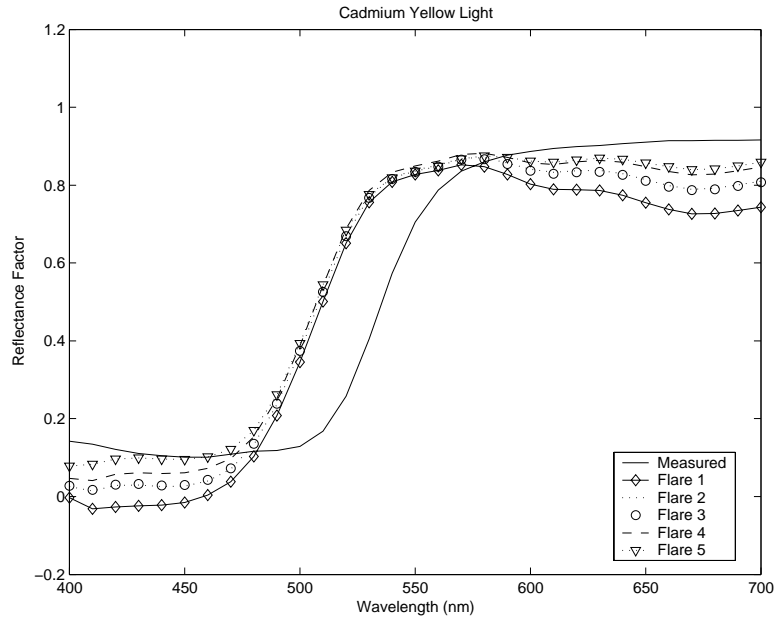
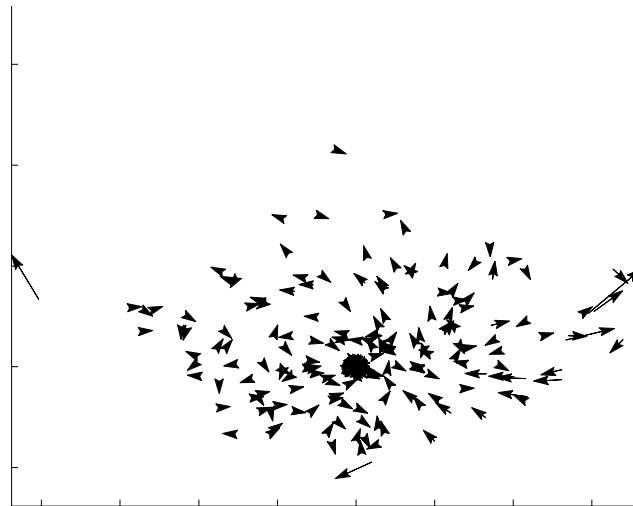


Figure 10b: Measured and Estimated Spectra of Cadmium Yellow Light

Colorimetric Evaluation:

There are no clearly defined metrics for flare or spectral estimation in general, but an analysis on colorimetric accuracy can serve as a good measure and gives some insight to the performance of the transformation matrix when flare is reduced. For this experiment, plots of the patches values in  $L^*a^*b^*$  coordinates and comparisons of the CIEDE2000 were used. Figure 11 shows changes between measured and estimated spectra using the transforms based on data from flare 1 and flare 5. While there are apparent differences for flare 1, flare 5 shows little if any change in colorimetric coordinates



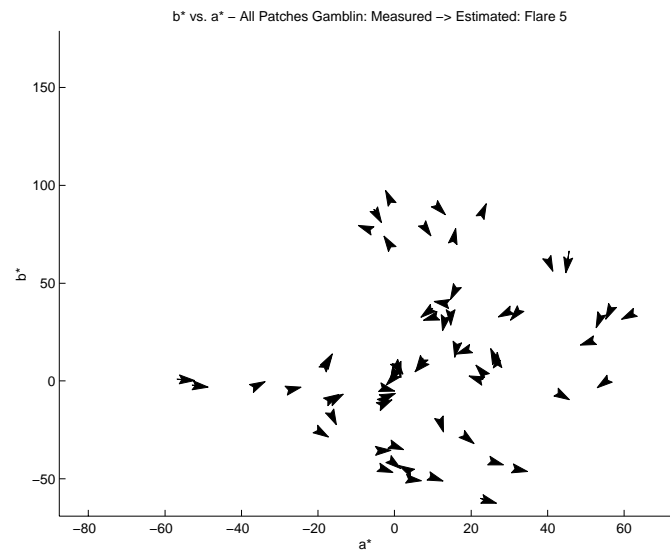
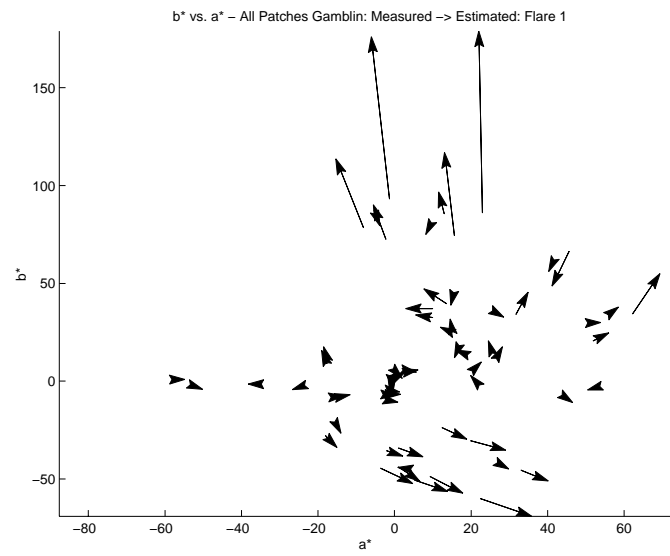
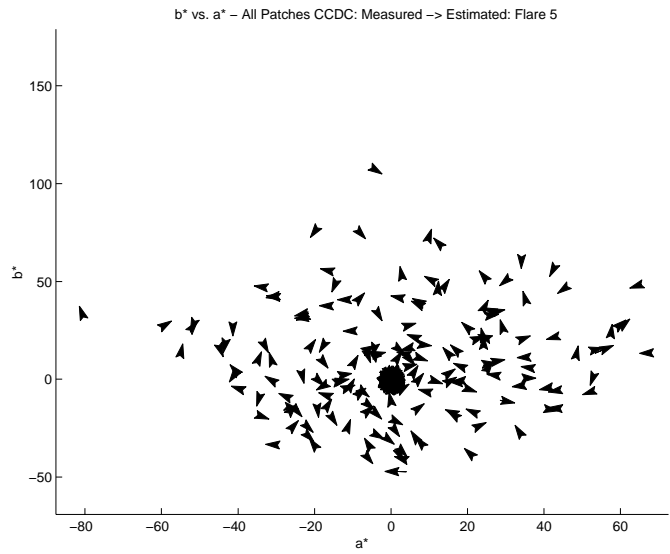


Figure 11:  $b^*$  vs.  $a^*$  for both CCDC and Gamblin patches

Histogram plots of the CIEDE2000 show that as the flare is reduced, the maximum CIEDE2000 decreases and in general, the patch's CIEDE2000 decreases (Figure 12).

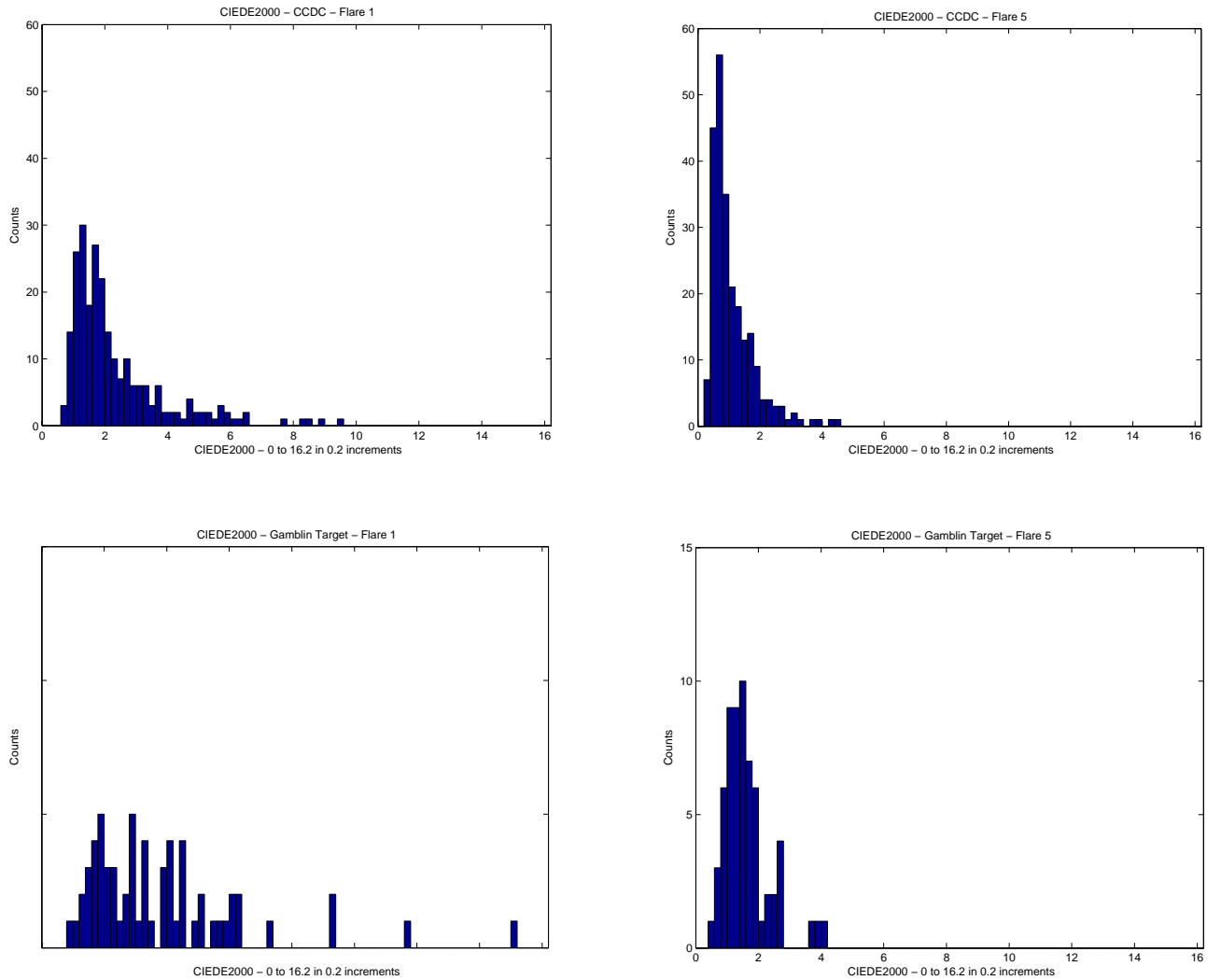


Figure 12: Histogram Plots of CIEDE 2000 for both data sets

### Quantification of Flare:

This report has so far considered the effects of flare on the transformation matrix and effects on the quality of spectral reflectance estimation, the flare has yet to be quantified to obtain some insight as to how it works and how it affects the digital output of the camera. König, *et al.* expressed the raw digital signal of a digital camera with the following equation:

$$d(x, y, i) = \int p_{\lambda} \cdot f_{\lambda, i} \cdot r_{\lambda}(x, y) \cdot s_{\lambda} d\lambda + \eta(x, y, t_{\text{exp}, i}) \quad (1.4)$$

where  $p_{\lambda}$  is the illuminant,  $f_{\lambda, i}$  is the transmittance of the  $i$ th spectral filter (or tuning wavelength in our case),  $r_{\lambda}(x, y)$  is the reflectance of the image,  $s_{\lambda}$  is the sensitivity of the sensor,  $x$  and  $y$  denote the pixel coordinates, and  $\eta$  is the fixed pattern noise for an exposure time  $t$  with filter  $i$ . If we try to calculate the digital count at zero reflectance, the integral term drops out and the equation is

simply the additive term for fixed pattern noise. Assuming that we can image an object with zero percent reflectance and that flare is proportionally linear with time, a flare term can be added to the equation:

$$d(x, y, i) = \eta(x, y, t_{exp, i}) + flare(x, y, i) \quad (1.5)$$

Thus, we can rearrange the terms and devise a way to quantify the flare in terms of digital counts.

$$flare(x, y, i) = d(x, y, i) - \eta(x, y, t_{exp, i}) \quad (1.6)$$

While zero percent reflectance data was not available at all wavelengths, there was data from two gray cards of different reflectances. Since digital counts can be thought of as a linear function of reflectance, zero percent reflectance could be extrapolated by finding the equation of the line that the average digital count for the central area of the gray cards lie on and then calculating for zero reflectance. This was done for the data at every wavelength imaged and then the values were plotted with the halon values and gray card values. It was expected that the flare would closely resemble the halon line in that it would be shifted since the flare light should have the same properties as the light reflecting off the halon. Figure 13 shows that while this is the case for wavelengths above 500 nm, there are still some problems in the lower wavelength bands.

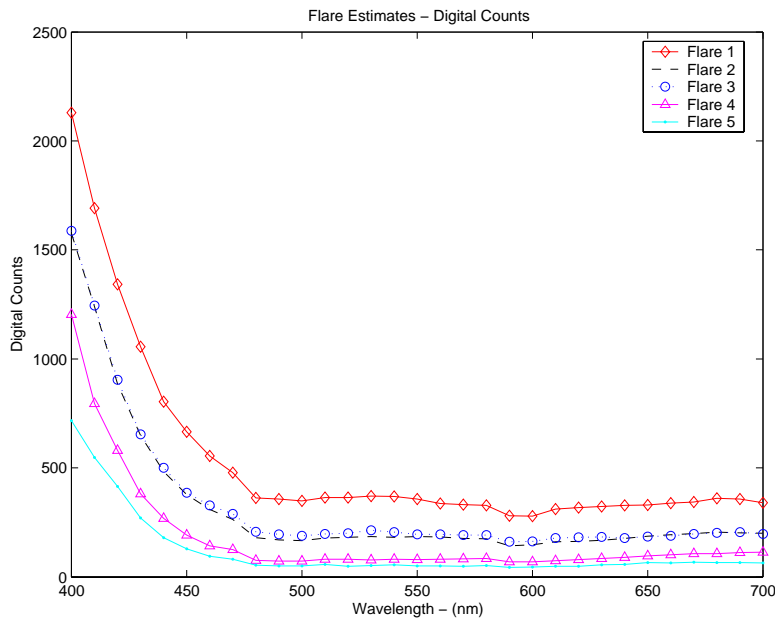


Figure 13: Flare Estimates at 400 – 700 nm for Flare 1-5

To observe how spatial uniformity may also affect the system, images of the gray cards before flat fielding were made. If the image were spatially uniform, there would be little color variation among the pixels in the image. Again, this was not the case in the lower and upper extremities of the sampled wavelengths, such as 400, 410, 420, and 700 nm. Figure 14 demonstrates this idea for the light gray card at flare 5, which is the best we would expect.

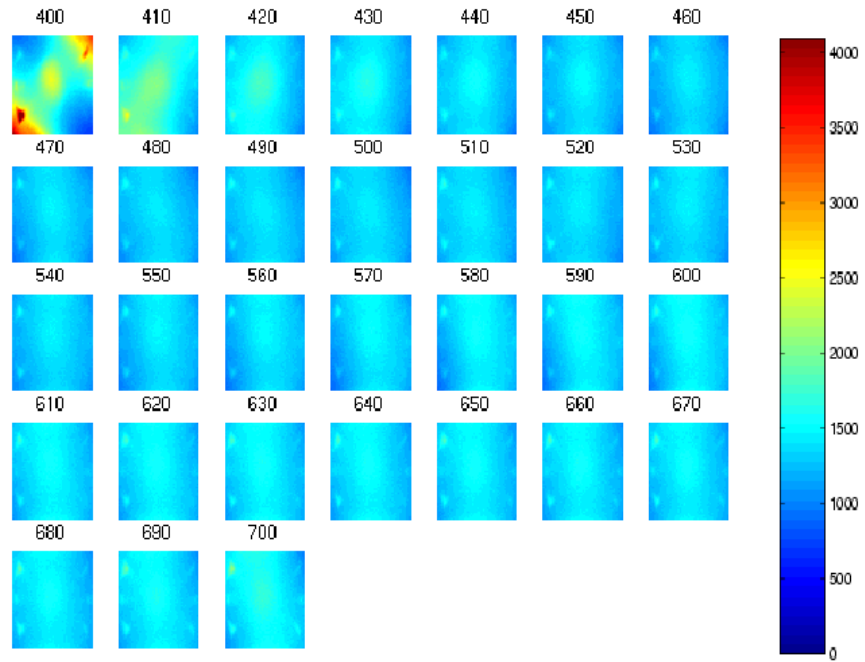


Figure 14: Image Uniformity of Light Gray Card (Flare 5)

Another way to try to observe the effect of spatial and the effect flare may have on the spectral estimation was to plot the RMS Spectral Error of the CCDC in a grid (Figure 15).

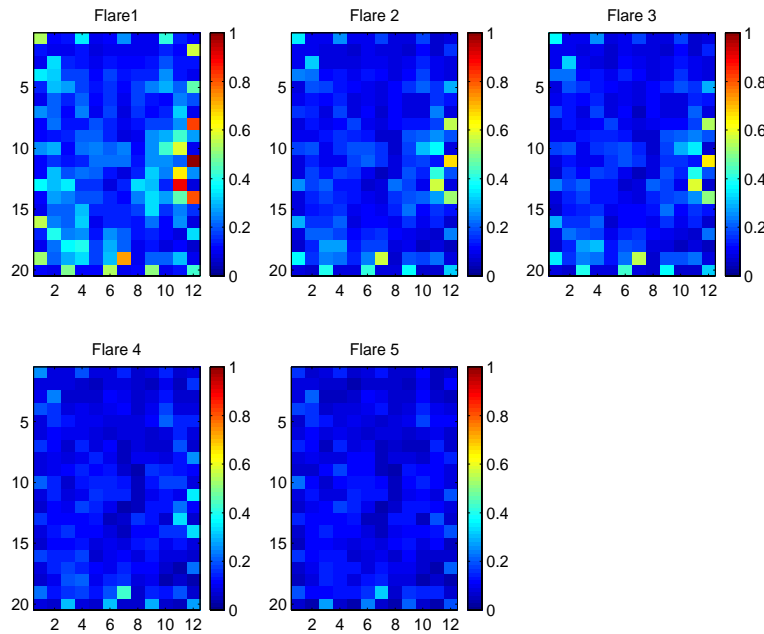


Figure 15: RMS Spectral Error plots

This shows the RMS error relative to position in the image. It should be noted that these images represent the top half of the target shown in Figure 2 rotated 90 degrees counter-clockwise. It was expected that the RMS error for the CCDC would be zero,

particularly around the outer edges, which are the same three color chips in a repeating pattern. While the error decreases with decrease in flare, the first level shows how nonuniformity in the center of the image (far right, center of Flare 1) can have a pronounced effect.

### **Discussion:**

It has been shown that a reduction in flare will improve the accuracy of estimated reflectance spectra, yet it is still not clear as to the manner that optical flare directly interacts with the transformation matrix. There are still several other factors involved in the image acquisition process that can also introduce uncertainty into the system. For example, inaccuracies are introduced by using the LCTF at certain wavelengths, which is a result of the LCTF not possessing uniform bandwidth properties. CRI specifies the nominal bandwidth at 550 nm while at other wavelengths the bandpass will vary with an approximately quadratic relationship to the centered wavelength. Also, there are variations in the filter as the light's angle of incidence changes - rays that are off axis can have a bandwidth that is shifted as much as 1/4 the ideal value towards the red region of the spectrum. Figure 16 gives measurements of spectral transmittance sampled in previous experiments with the LCTF when tuned to 400, 450, 550, 650, and 700 nm, showing the increase in bandpass as wavelength increases.

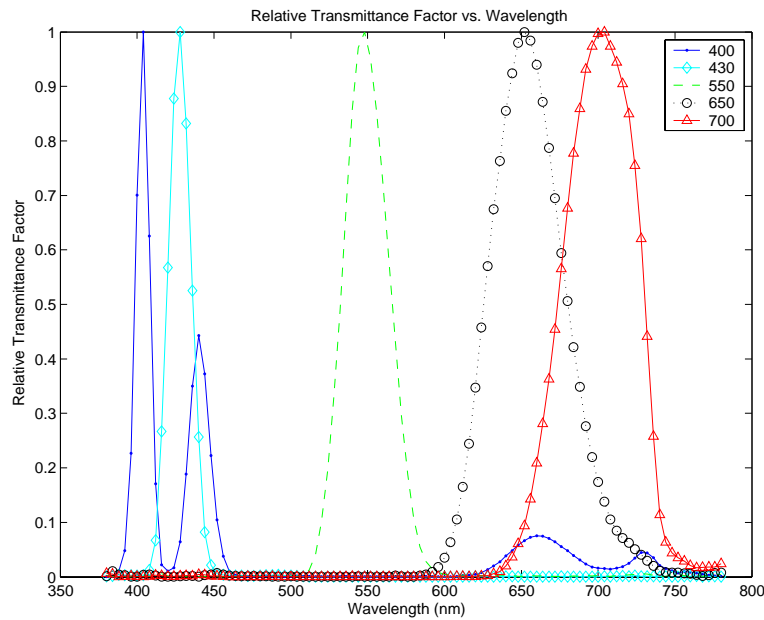


Figure 16: LCTF Bandpass at Selected Wavelengths

Ideally, the multiplication of the camera sensitivity and the transmittance of the filter should yield a triangular sampling function with 10nm bandpass. Figure 17 shows the normalized sampling functions at different wavelengths, showing where error may be introduced into the system.

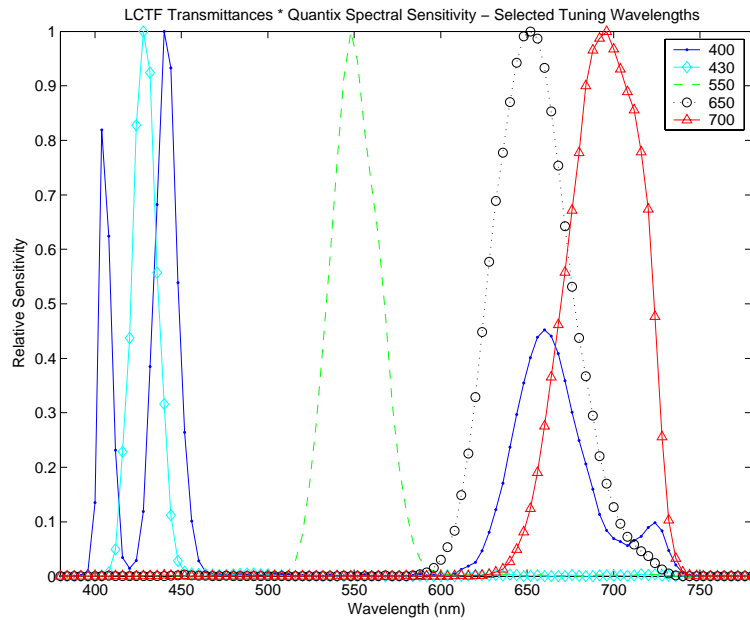


Figure 17: Sampling Curves

Also, the angle of incidence of the light with the tunable filter has an effect on the transmittance that affects the accuracy of the output. As stated earlier, the angle of incidence of light initially hitting the LCTF can have an effect on the transmittance, but also the pixel position of the CCD relative to the filter will affect the final estimate. The angular dependence was empirically observed by simply tuning the wavelength to a given frequency and then tilting it and observing the color shift. Previous experiments by König *et al.* have shown that an angle of incidence of 15 degrees. can add as much as  $2 \Delta E_{ab}$ . Also, a lack of coplanarity can cause significant error in a system. While the reference (König, *et al.*) example based on the use of interference filters, the LCTF may not be entirely uniform across the glass surface, and flare light is incident at angles different from off axis lighting. While a possibility, nonuniformity across the surface of the filter is most likely much less prevalent than the effects of light incident at different angles. Finally, a factor that may be generating significant system noise is cross coupling between pixels (König, *et al.*). This is generally caused by interreflections within the lens, from the LCTF, etc. It should be noted that the casing and inner components of the lens/LCTF combination are not mat, but in fact have dark polished surfaces which may give some specular reflections. These are only some of the sources of error, and it will most likely be impossible to eliminate all sources of error. The most important question is what degree of error is considered acceptable and what factors can be minimized or eliminated to arrive within that acceptable error level?

### **Conclusions:**

An evaluation of flare has been undertaken to try and understand some of the effects it may have on a system and its contributions to the noise of the system. Several metrics and methods were used in trying to quantify flare in different ways and to quantify the quality of the resulting spectral estimation. Some of the advantages and weaknesses of the present system as well as other sources of

error were discussed. While the direct relationship between optical flare and the transformation matrix could not be determined, it was shown that an overall reduction in flare light from the scene will improve the spectral reflectance estimates from the system.

It was necessary to perform this experiment for several reasons:

- To begin to look at ways to quantify flare and further refine methods of removing it.
- To understand that it is important to use good imaging practices at the beginning of the imaging chain (image capture). In general, when input data are good, quality output is achieved in a much easier manner.
- To look at other sources of error and realize that it is important to try and understand as many aspects of the system as possible to improve output quality.
- To gain a greater appreciation for the complexity of the task at hand.

Future experiments could include:

- An investigation of methods to further improve the quantization of flare.
- An examination of the effects of angles of incidence and methods to remove them if necessary.
- Experiments on methods to isolate/reduce/or eliminate effects due to factors such as cross coupling and further characterize flare in a system.

## **References:**

- [1] Stroebel, Leslie, et al., Basic Photographic Materials and Processes, Focal Press (1990).
- [2] Imai, Francisco H., et al. "Technical Report: Comparison of the accuracy of various transformations from multi-band images to reflectance spectra" - [www.art-si.org](http://www.art-si.org) (2000).
- [3] König, Friedhelm and Werner Praefcke. "The Practice of Multispectral Image Acquisition", Proceedings: Europto Confrence on Electronic Imaging, Processing, Printing, and Publishing in Color}, Zurich, Switzerland (1998)
- [4] CRI Tech Support Document - VariSpec Wavelength Accuracy, Bandwidth, Tuning Accuracy - [www.cri-inc.com](http://www.cri-inc.com)